Journal of Mathematical Control Science and Applications
Vol. 3 No. 2 (July-December, 2017)

Submitted: 24th September 2017 *Revised: 19th December 2017* *Accepted: 30th December 2017*

HEAT AND MASS TRANSFER CHARACTERISTICS OF CASSON FLUID OVER A DISK IN POROUS MEDIA WITH VARIABLE THERMAL CONDUCTIVITY

S. PRASANNA RANI

ABSTRACT. The present research investigates the flow, heat and mass transfer characteristics of a Casson fluid over a reciprocating disk, taking into account the impact of variable thermal conductivity, porous media and chemical reactions. The Casson constitutive relation represents the non-Newtonian character of the fluid, while the porous media adds resistance to fluid flow. The governing partial differential equations for momentum, energy and concentration are converted into a system of coupled nonlinear ordinary differential equations using suitable similarity transformations. The resultant equations are numerically solved using the Runge-Kutta-Fehlberg fourth-fifth (RKF-45) technique. The Casson parameter, porous-medium parameter, thermal conductivity parameter, chemical reaction parameter and reciprocating disk features all have a significant impact on the velocity, temperature and concentration profiles. The findings show that increasing porous-medium resistance lowers fluid velocity, but increased thermal conductivity considerably modifies the thermal boundary layer. Furthermore, the chemical reaction parameter is critical for identifying a species concentration within the flow field. The present research gives valuable insights for applications in chemical processing, thermal systems and energy-related technologies, as well as a greater knowledge of transfer processes in reactive non-Newtonian fluids moving through porous media.

1. Nomenclature

Symbols	**Descriptions**	**Symbols**	**Descriptions**
$\kappa(T)$	Variable thermal conductivity	D_m	Mass diffusivity
$b(t)$	Distance	β	Casson parameter
ρ	Density	C_p	Specific heat
k	Thermal conductivity	T_d	Disk surface temperature
T	Temperature	T_∞	Ambient temperature
C	Concentration	k_0	Reaction rate
Pr	Prandtl number	(U, V, W)	Dimensionless velocity
p	Pressure	ν	Kinematic viscosity
Sc	Schmidt number	M	Porosity parameter
ϖ_d	Rotational characteristic of disk	ϖ_f	Rotational characteristic of fluid
S	Vertical reciprocation parameter of disk	$\omega(t)$	Rotational motion of disk
$\Omega(t)$	Rotational motion of fluid	ε	Variable thermal conductivity parameter

2000 *Mathematics Subject Classification.* 76S05, 80A20.
Key words and phrases. Reciprocating disk; Casson fluid; Porous media; Variable thermal conductivity; Chemical reaction.

2. Introduction

The flow through a disk is a major area of research from both engineering and mathematical points of view that attracts many researchers nowadays. A circular, flat component in a laboratory setup that travels continuously in the vertical direction is referred to as a Reciprocating disk. This periodic motion produces an unsteady hydrodynamic force and controlled vortex dynamics. The flow through a reciprocating disk is of major concern due to its applications in the generation of power, rotating cleaning machines, humidifiers, aircraft engines and medical and electrochemical equipment. Komoda et al. [5] studied the laminar flow induced by a reciprocating disk. Hirata et al. [4] studied a reciprocating disk, showing that periodic disk movement creates vortices and chaotic mixing. Pei et al. [11] deliberated the reciprocating angular movement of a suspension–slider system.

Researchers are interested in unsteady non-Newtonian liquid flow having a definite yield value due to their usefulness in polymer processing industries and biofluid dynamics. Among these, the unsteady flow of a non-Newtonian Casson fluid is an important one and is defined as a shear-thinning liquid having infinite viscosity at zero shear rate. Different experiments were conducted on blood with varying temperatures and anticoagulants and showed that the blood behaves like a Casson fluid. Casson fluids behave like solids when the applied force is low, and they become fluids when pushed harder. Due to this, they are vital in medicines and in synthetic polymers. Mukhopadhyay et al. [9] investigated the two-dimensional, unsteady flow of a Casson fluid past a stretching sheet. Pramanik [12] examined the flow of a Casson fluid past a stretching surface with suction and blowing effects. Ramesh and Devakar [13] analysed the impacts of slip condition on the flow of a Casson fluid.

Porous media are materials that consist of small holes through which liquid or gas particles move. Porous media are made up of different minerals, and their scale varies from nm to m. The special property of a porous material is that it is capable of differentiating it from other solid materials. Porous materials are good thermal insulators due to their porous nature. The flow through porous media has several engineering applications, such as filtration, catalytic chemical reactions, powder metallurgy, aerospace, petroleum and mechanical engineering. Sochi [15] studied the non-Newtonian fluid flow through porous media. Arpino et al. [1] examined the porous medium-free fluid interface model with a high source term. Mahdi et al. [8] addressed the flow and convective heat transfer of fluid in porous media.

The property of a material that changes due to variations in temperature. Thermal conductivity depends purely on the nature of the material, and it is important in cooling technology. Thermal conductivity is a fundamental parameter for heat transfer in fluids. The study of variable thermal conductivity is vital in electrolytes due to its use in the preparation of batteries. Variable thermal conductivity heat transfer has many engineering applications, like industrial cooling systems, polymer extraction and processing, petroleum transport and heat exchangers. Lin et al. [6] investigated the impacts of variable thermal conductivity and thermal radiation on the flow of nanofluid. Reddy [3] analysed the impacts of variable thermal conductivity on the flow of a Casson fluid with thermal radiation. Lin et al. [7] examined the flow of a nanofluid subjected to the impacts of variable thermal conductivity and viscous dissipation.

Chemical reaction refers to the combination of two or more elements to form a single compound. In this process, reactants are converted into products. A Chemical reaction is said to be of first order if the reaction rate is proportional to the concentration of the fluid. A chemical reaction always yields a chemical change and a product having behaviours different from the reactant. Some chemical reactions generate heat, called exothermic reactions, and some chemical reactions require heat, called endothermic reactions. Chemical reactions have many industrial applications, including polymer production, food processing and oxidation of solid materials. Patil and Kulkarni [10] studied the mass and heat transfer in a two-dimensional, time-independent, laminar flow of a polar fluid across a porous medium subjected to chemical reaction and internal heat generation effects. Damesh et al. [2] investigated the mass and heat transfer in a viscous, micropolar fluid flow subjected to the impact of a first-order chemical reaction past a permeable surface. Shehzad et al. [14] considered the impact of chemical reaction on the Casson fluid flow past a stretching porous sheet to elaborate on the heat and mass transfer.

The current study investigates the flow, heat and mass transfer properties of a Casson fluid over a reciprocating disk, taking into account the combined impacts of variable thermal conductivity, porous media and chemical reaction. Although Casson fluid flow over stretching and rotating surfaces has been extensively studied, there are still limited studies that address reciprocating disk movement along with temperature-dependent thermal conductivity and porous resistance. A more accurate representation of heat transfer in high-temperature industrial processes, where fluid characteristics significantly alter with temperature, is made possible by the inclusion of variable thermal conductivity. Additionally, the chemical reaction parameter allows for the measurement of reactive species movement in catalytic and chemical engineering systems. The interaction of non-Newtonian rheology, porous-medium permeability, variable thermal conductivity and chemical kinetics reveals novel information about momentum, thermal and concentration boundary-layer behaviour. The findings of this study are useful for building advanced thermal management systems, chemical reactors, filtration units and energy-conversion devices that use reactive non-Newtonian fluids.

3. Mathematical analysis

For the current study, the axisymmetric Casson fluid past an infinite reciprocating rotating disk is discussed. Cylindrical coordinates $(r,\,\phi,\,z)$ are used, which are the radial, azimuthal and axial coordinates, respectively. The disk is located at the coordinate $z = b\,(t)$, where $b\,(t)$ represents its current vertical position. This means that the vertical speed of the disk is $w = \frac{\partial b(t)}{\partial t}$. The disk also moves with an angular speed of $\omega\,(t)$. The fluid far from the disk is maintained at a constant ambient temperature T_∞, whereas the disk surface temperature $T_d\,(t)$ is assumed to vary with time due to the vertical movement of the disk. It is defined as:

$$T_d\,(t) = T_\infty + \frac{c}{\left(b\,(t)\right)^{2a}}.$$

Where c is an arbitrary constant and a is the wall temperature parameter. The case $a = 0$ corresponds to a constant surface temperature, while $a \neq 0$ represents a time-dependent thermal boundary condition influenced by the disk motion. The governing equations are as follows:

$$\frac{\partial u}{\partial r} + \frac{\partial w}{\partial z} + \frac{u}{r} = 0, \tag{1}$$

(2)
$$\frac{\partial u}{\partial t}+\left[u\frac{\partial u}{\partial r}+w\frac{\partial u}{\partial z}-\frac{v^2}{r}\right]+\frac{1}{\rho}\frac{\partial p}{\partial r}-2\Omega v=\nu\left(1+\frac{1}{\beta}\right)\left[\frac{\partial^2 u}{\partial z^2}+\frac{\partial^2 u}{\partial r^2}-\frac{u}{r^2}+\frac{1}{r}\frac{\partial u}{\partial r}\right]-\frac{\nu}{K}u,$$

(3) $$\frac{\partial v}{\partial t}+\left[u\frac{\partial v}{\partial r}+w\frac{\partial v}{\partial z}-\frac{uv}{r}\right]+2\Omega u=\nu\left(1+\frac{1}{\beta}\right)\left[\frac{\partial^2 v}{\partial z^2}+\frac{\partial^2 v}{\partial r^2}-\frac{v}{r^2}+\frac{1}{r}\frac{\partial v}{\partial r}\right]-\frac{\nu}{K}v,$$

(4) $$\frac{\partial w}{\partial t}+\left[u\frac{\partial w}{\partial r}+w\frac{\partial w}{\partial z}\right]+\frac{1}{\rho}\frac{\partial p}{\partial z}=\nu\left(1+\frac{1}{\beta}\right)\left[\frac{\partial^2 w}{\partial z^2}+\frac{\partial^2 w}{\partial r^2}+\frac{1}{r}\frac{\partial w}{\partial r}\right]-\frac{\nu}{K}w,$$

(5) $$\begin{aligned}&(\rho C_p)\left[\tfrac{\partial T}{\partial t}+u\tfrac{\partial T}{\partial r}+w\tfrac{\partial T}{\partial z}\right]-\tfrac{\partial T}{\partial r}\left[\tfrac{\partial \kappa(T)}{\partial r}\right]\\&\qquad=\kappa(T)\left[\tfrac{\partial^2 T}{\partial z^2}+\tfrac{\partial^2 T}{\partial r^2}+\tfrac{1}{r}\tfrac{\partial T}{\partial r}\right]+\tfrac{\partial T}{\partial z}\left[\tfrac{\partial \kappa(T)}{\partial z}\right],\end{aligned}$$

(6) $$\frac{\partial C}{\partial t}+u\frac{\partial C}{\partial r}+w\frac{\partial C}{\partial z}=D_m\left[\frac{\partial^2 C}{\partial z^2}+\frac{\partial^2 C}{\partial r^2}+\frac{1}{r}\frac{\partial C}{\partial r}\right]-k_0\left(C-C_\infty\right).$$

Where,

(7) $$\kappa(T)=k\left(\frac{T_d-T_\infty+\varepsilon\left(T-T_\infty\right)}{T_d-T_\infty}\right).$$

Corresponding boundary conditions are:

(8) $$\left.\begin{array}{l}u=0,\, v=\omega r,\, w=\delta\frac{\partial b(t)}{\partial t},\, T=T_d,\, C=C_d,\ \ at\ \ z=b(t)\\ u=0,\, v=\Omega r,\, T=T_\infty,\, C=C_\infty,\ \ as\ \ z\to\infty.\end{array}\right\}$$

Similarity variables:

(9) $$\left.\begin{array}{l}u=\frac{r\nu U}{b^2(t)},\, v=\frac{r\nu V}{b^2(t)},\, w=\frac{\nu W}{b(t)},\, \eta=\frac{z}{b(t)}-1,\\ T=T_\infty+\left(T_d-T_\infty\right)\theta,\, C=C_\infty+\left(C_d-C_\infty\right)\chi,\, p=\frac{\rho\nu P}{b^2(t)}.\end{array}\right\}$$

Reduced governing equation:

$$2U+W'=0,$$

(10) $$\left(1+\frac{1}{\beta}\right)U''-\left[U^2-V^2+U'W-2\varpi_f V-S\left(\frac{(\eta+1)}{2}U'+U\right)\right]-\varpi_d MU=0,$$

(11) $$\left(1+\frac{1}{\beta}\right)V''-\left[2UV+WV'+2\varpi_f U-S\left(\frac{(\eta+1)}{2}V'+V\right)\right]-\varpi_d MV=0,$$

(12) $$P'-\left[\left(1+\frac{1}{\beta}\right)W''-\varpi_d MW\right]-\frac{S}{2}\left[(\eta+1)W'+W\right]+WW'=0,$$

(13) $$(1+\varepsilon\theta)\theta''+\Pr\left[\frac{S}{2}(\eta+1)\theta'+aS\theta-W\theta'\right]+\varepsilon\left(\theta'\right)^2=0,$$

(14) $$\chi''+\frac{(\eta+1)}{2}ScS\chi'-ScW\chi'-ScK_r\varpi_d\chi=0,$$

Boundary conditions are:

(15) $$\left.\begin{array}{ll}U=0,\, V=\varpi_d,\, W=\delta\frac{S}{2},\, \theta=1,\, \chi=1, & at\ \ \eta=0\\ U=0,\, V=\varpi_f,\, \theta=0,\, \chi=0, & as\ \ \eta\to\infty.\end{array}\right\}$$

Where,

$$\left.\begin{array}{l} S = \frac{2b(t)\frac{\partial b(t)}{\partial t}}{\nu},\ \Pr = \frac{(\rho C_p)\nu}{k},\ \varpi_f = \frac{\Omega(t)b^2(t)}{\nu}, \\ \varpi_d = \frac{\omega(t)b^2(t)}{\nu},\ M = \frac{\nu}{\omega(t)K},\ Sc = \frac{\nu}{D_m},\ \beta = \frac{\lambda^*\nu}{b^2(t)}. \end{array}\right\} \tag{16}$$

4. Methodology

The RKF-45 approach was used to numerically solve the system of coupled nonlinear ordinary differential equations that were derived using similarity transformations. The RKF-45 scheme is an adaptive step-size integration method that automatically modifies the step size for increased accuracy and computational efficiency while concurrently computing fourth- and fifth-order approximations to estimate the local truncation error. In order to solve the transformed boundary value problem with the specified boundary conditions, it was first transformed into an equivalent system of first-order differential equations. Until the convergence criterion of 10^{-6} was fulfilled, iterative calculations were carried out. The RKF-45 method is especially useful for analyzing the current flow, heat, and mass transfer problem involving Casson fluid dynamics, porous-medium effects, variable thermal conductivity, and chemical reactions because of its stability, dependability, and high accuracy in handling strongly nonlinear systems.

$$\left.\begin{array}{l} W = \Gamma_1,\ U = \Gamma_2,\ U' = \Gamma_3,\ V = \Gamma_4, V' = \Gamma_5, \\ \theta = \Gamma_6,\ \theta' = \Gamma_7,\ \chi = \Gamma_8,\ \chi' = \Gamma_9. \end{array}\right\} \tag{17}$$

$$\Gamma_1' = -2\Gamma_2, \tag{18}$$

$$\Gamma_3' = \frac{1}{\left(1+\frac{1}{\beta}\right)}\left[{\Gamma_2}^2 - {\Gamma_4}^2 + \Gamma_3\Gamma_1 - 2\varpi_f\Gamma_4 - S\left(\frac{(\eta+1)}{2}\Gamma_3 + \Gamma_2\right)\right] - \varpi_d M\Gamma_2, \tag{19}$$

$$\Gamma_5' = \frac{1}{\left(1+\frac{1}{\beta}\right)}\left[2\Gamma_2\Gamma_4 + \Gamma_1\Gamma_5 + 2\varpi_f\Gamma_2 - S\left(\frac{(\eta+1)}{2}\Gamma_5 + \Gamma_4\right)\right] - \varpi_d M\Gamma_4, \tag{20}$$

$$\Gamma_7' = -\frac{1}{(1+\varepsilon\theta)}\left[\Pr\left[\frac{S}{2}(\eta+1)\Gamma_7 + aS\Gamma_6 - \Gamma_1\Gamma_7\right] + \varepsilon(\Gamma_7)^2\right], \tag{21}$$

$$\Gamma_9' = -\frac{(\eta+1)}{2}ScS\Gamma_9 + Sc\Gamma_1\Gamma_9 + ScK_r\varpi_d\Gamma_8, \tag{22}$$

Boundary conditions are:

$$\left.\begin{array}{l} \Gamma_2 = 0,\ \Gamma_4 - \varpi_d = 0,\ \Gamma_1(0) - \delta\frac{S}{2} = 0,\ \Gamma_6(0) - 1 = 0,\ \Gamma_8(0) - 1 = 0, \\ \Gamma_2(\infty) = 0,\ \Gamma_4(\infty) - \varpi_f = 0,\ \Gamma_6(\infty) = 0,\ \Gamma_8(\infty) = 0. \end{array}\right\} \tag{23}$$

5. Result and discussion

The transformed governing equations describing the momentum, energy, and concentration transfer of a Casson fluid over a vertically reciprocating disk were numerically solved using the RKF-45 technique. This section presents and discusses how the radial velocity, tangential velocity, temperature, and concentration profiles are affected by the several parameters. The graphical findings show how the governing parameters affect the flow's hydrodynamic, thermal, and mass transfer properties and give a thorough understanding of the underlying transport mechanisms. The interaction of fluid rheology, porous-medium resistance, thermal diffusion, and species transport mechanisms is used to evaluate the physical significance of the observed patterns.

Figure 1 shows the effect of the Casson parameter β on radial velocity $U(\eta)$. Increasing β from 0.1 to 0.9 significantly lowers the radial velocity over the boundary layer. Higher β values lead to a decrease in peak velocity near the disk surface and a faster approach to the ambient condition. A higher Casson parameter increases the fluid's resistance to deformation, resulting in more viscous effects that prevent momentum from flowing radially. As a result, the thickness of the momentum boundary layer decreases, causing the reciprocating disk-induced radial flow to decrease. Figure 2 shows the impact of the porosity parameter M on the radial velocity $U(\eta)$. The radial velocity drops significantly as M grows from 0.3 to 1.5. The highest velocity near the disk surface decreases, and the velocity profiles decline more rapidly as M increases. A higher porosity value increases the resistance provided by the porous medium, reducing fluid velocity and decreasing radial momentum transfer. As a result, the momentum boundary layer becomes thin, reducing the radial flow generated by the reciprocating disk. Thus, raising M slows fluid velocity over the flow domain. Figure 3 shows the effect of the vertical reciprocation parameter S on the radial velocity $U(\eta)$. Radial velocity rises with S values from -0.3 to 0.3. The peak velocity at the disk surface increases, but the velocity profiles stay high across the boundary layer area. Positive vertical reciprocation increases momentum transfer from the oscillating disk to the surrounding fluid, which accelerates radial flow. As a result, the thickness of the momentum boundary layer rises, causing greater radial flow. Thus, the vertical reciprocation parameter serves as a driving mechanism, promoting fluid movement and improving radial velocity.

Figure 4 shows the impact of the Casson parameter β on the tangential velocity $V(\eta)$. Tangential velocity decreases with higher values of β. The velocity profiles show a monotonic decline from the disk surface and approach 0 further away from the disk. A larger Casson value enhances the fluid's resistance to deformation, reducing the rotational motion caused by the disk. As a result, the transfer of angular momentum from the disk to the fluid diminishes, resulting in a slower tangential velocity and a smaller momentum boundary layer. Increasing β decreases the swirling motion of the Casson fluid. Figure 5 shows the effect of the porosity parameter M on the tangential velocity $V(\eta)$. As M increases, $V(\eta)$ falls dramatically. This is due to increased resistance from the porous medium, which inhibits the fluid's rotation caused by the disk. As a result, the transfer of angular momentum diminishes, lowering the tangential velocity throughout the boundary layer. As a result, the thickness of the momentum boundary layer reduces, and the fluid reaches the quiescent state more quickly as M increases. Figure 6 shows how the vertical reciprocation parameter S affects tangential velocity $V(\eta)$. It is clear that raising S improves tangential velocity across the boundary layer area. The disk's oscillatory motion adds momentum to the fluid, improving rotational flow and angular momentum transfer. As a result, raising S causes the tangential velocity profiles to move upward and decay more slowly. This behaviour suggests a thickening of the momentum boundary layer and a greater swirling motion of the fluid as a result of increased vertical reciprocation.

Figure 7 shows how the variable thermal conductivity parameter ε affects the temperature distribution $\theta(\eta)$. The temperature profile clearly increases with rising ε values. As ε rises, the fluid's heat conduction improves. This allows thermal energy to move more efficiently from the heated disk into the surrounding fluid. As a result, greater temperatures are maintained across the thermal boundary layer, increasing its thickness.

As a result, the variable thermal conductivity parameter stimulates heat transfer and improves the temperature field inside the flow domain. Figure 8 shows how the temperature profile $\theta(\eta)$ varies with the vertical reciprocation parameter S. The temperature falls as S increases from -0.1 to 0.1. Stronger vertical reciprocation improves fluid mixing and more effectively transfers thermal energy away from the disk surface. This greater convective cooling decreases the thermal energy retained inside the boundary layer, resulting in lower temperatures over the flow area. As a result, the thickness of the thermal boundary layer reduces as S increases, showing that the temperature field is suppressed due to enhanced disk reciprocation.

Figure 9 shows the effect of the chemical reaction parameter K_r on the concentration profile $\chi(\eta)$. It is noticed that when K_r increases, the concentration reduces dramatically. A greater chemical reaction increases the consumption of diffusing species, lowering the concentration level within the boundary layer. As a result, concentration profiles decrease faster and approach the ambient state for lower values of η. As a result, the concentration boundary layer thickness falls as K_r increases, suggesting that the chemical reaction restricts species diffusion and mass movement in the fluid. Figure 10 demonstrates the way the concentration profile $\chi(\eta)$, varies with the Schmidt number Sc. It is clear that concentration drops as Sc increases from 0.3 to 1.5. Because the Schmidt number measures the ratio of momentum diffusivity to mass diffusivity, higher Sc values indicate lower species diffusivity. As a result, the diffusion of chemical species away from the disk surface is decreased, resulting in lower concentration levels across the boundary layer. As a result, increasing Sc thins the concentration boundary layer and lowers mass transfer inside the flow domain.

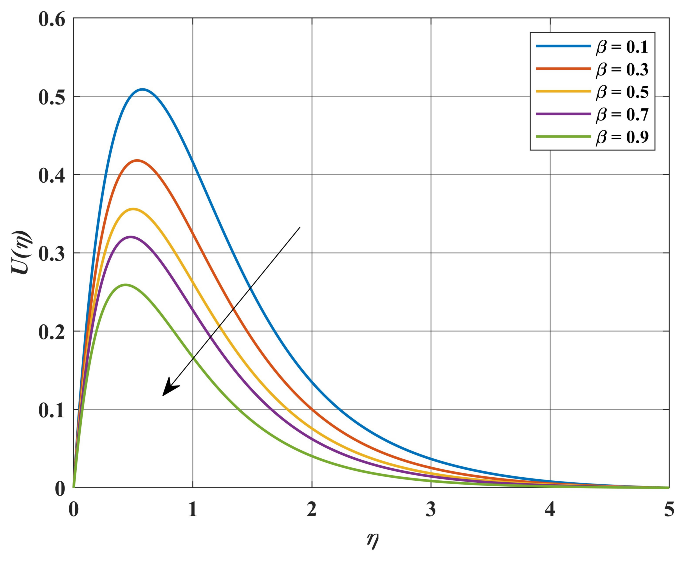

FIGURE 1. Impact of β on $U(\eta)$.

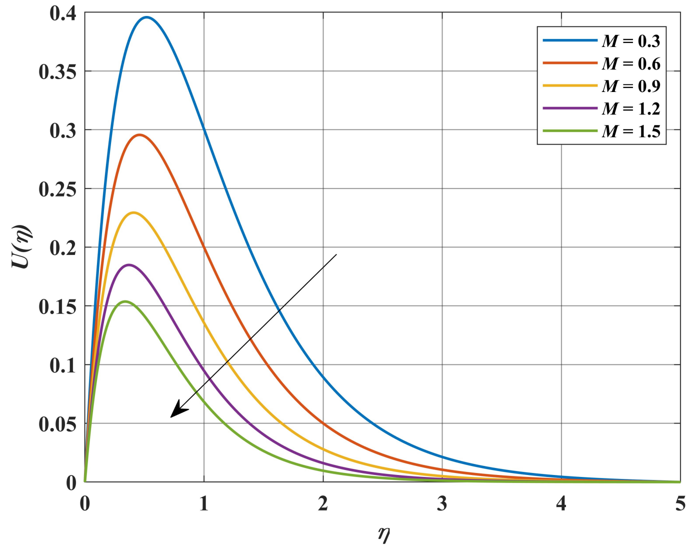

FIGURE 2. Impact of M on $U(\eta)$.

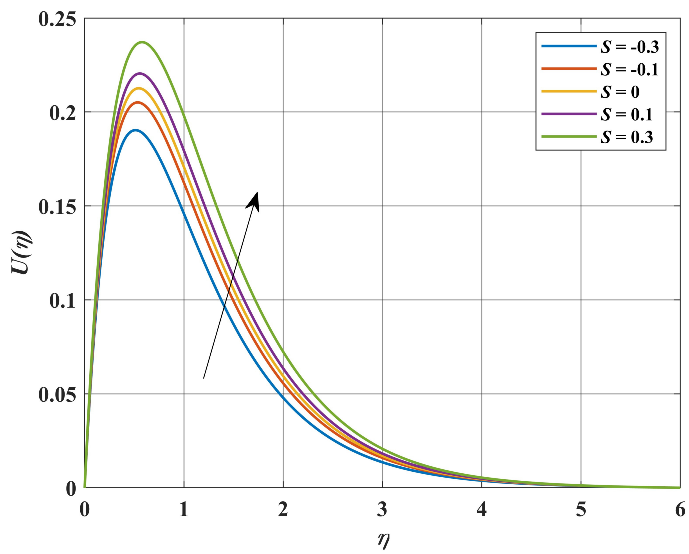

FIGURE 3. Impact of S on $U(\eta)$.

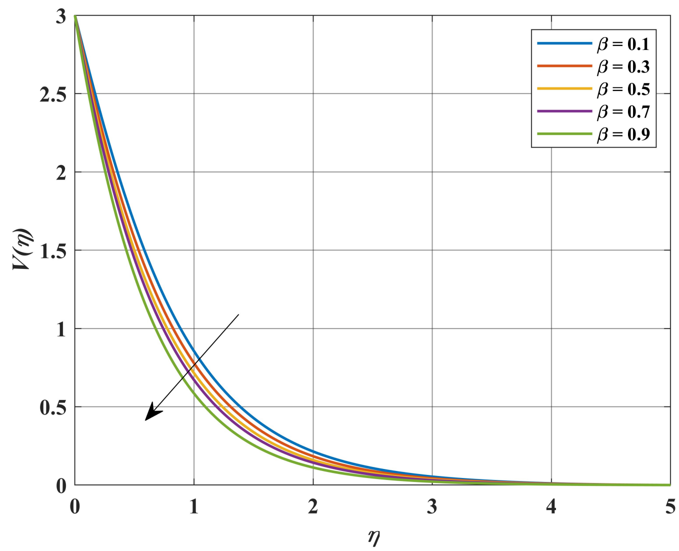

FIGURE 4. Impact of β on $V(\eta)$.

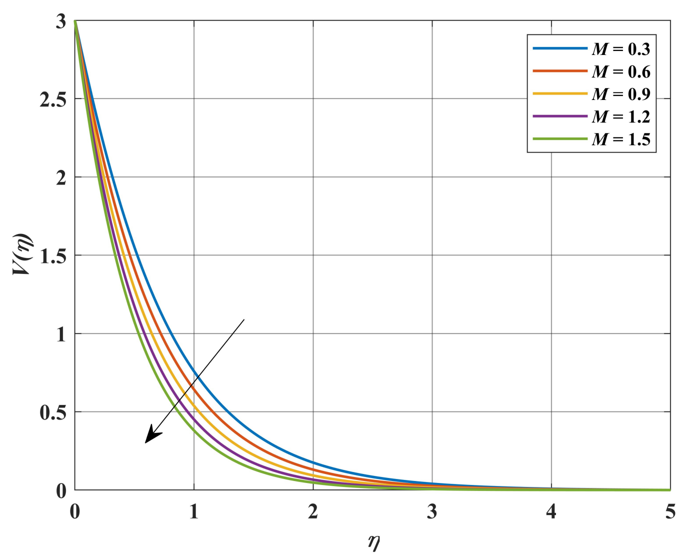

FIGURE 5. Impact of M on $V(\eta)$.

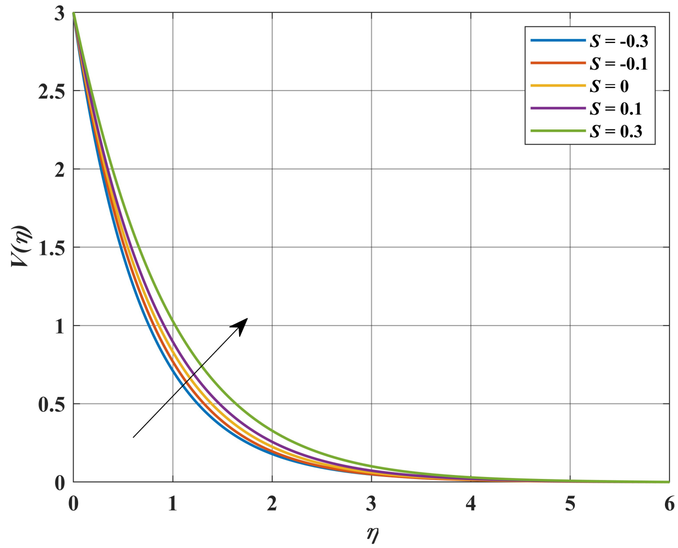

FIGURE 6. Impact of S on $V(\eta)$.

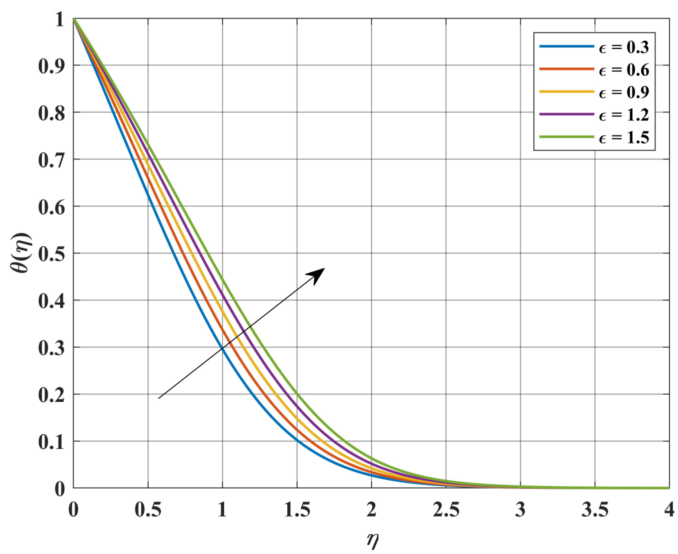

FIGURE 7. Impact of ε on $\theta(\eta)$.

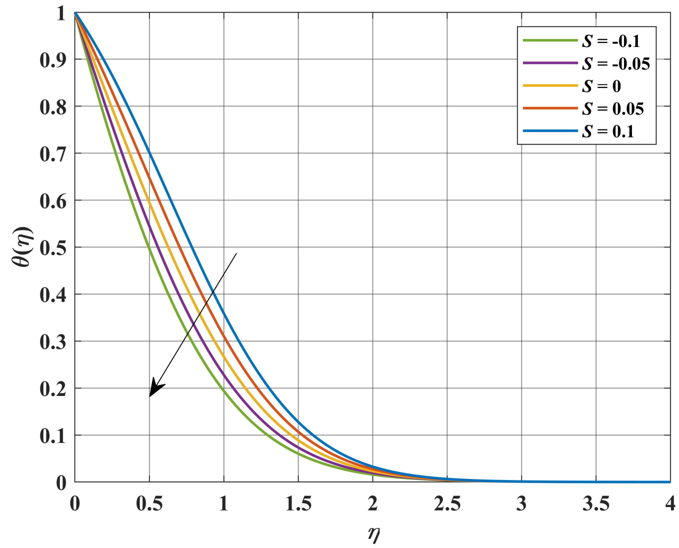

FIGURE 8. Impact of S on $\theta(\eta)$.

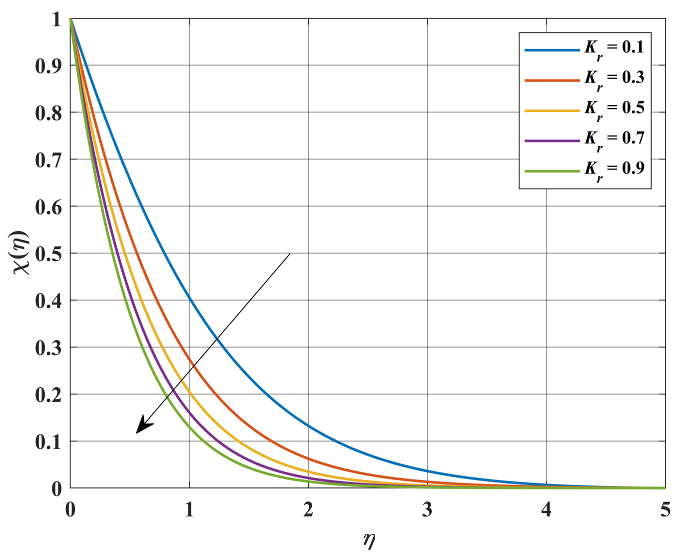

FIGURE 9. Impact of K_r on $\chi(\eta)$.

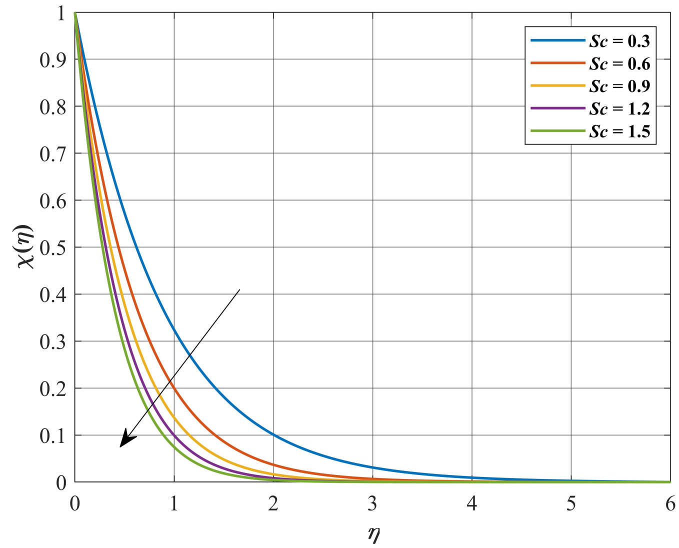

FIGURE 10. Impact of Sc on $\chi(\eta)$.

6. Conclusion

The current study examined the flow, heat and mass transfer properties of a Casson fluid generated by a vertically reciprocating disk in a porous medium with variable thermal conductivity and chemical reaction effects. The governing partial differential equations were converted to nonlinear ordinary differential equations using similarity transformations and numerically solved using the RKF-45 technique. The effects of the Casson parameter, porous-medium parameter, reciprocation parameter, variable thermal conductivity parameter, chemical reaction parameter and Schmidt number on transport properties were thoroughly investigated. The study's key findings are summarized as follows.

- Increasing the Casson parameter decreases both radial and tangential velocity profiles because it increases fluid deformation resistance.
- The porous-medium parameter lowers radial and tangential velocities by increasing drag force inside the porous region.
- Higher values of the vertical reciprocation parameter increase radial and tangential velocities by introducing momentum to the fluid.
- The variable thermal conductivity parameter improves temperature dispersion and thickens the thermal boundary layer.
- An increase in the vertical reciprocation parameter lowers the temperature profile due to improved convective transport and cooling.
- The chemical reaction parameter reduces the concentration profile by accelerating the consumption of the diffusing species.

- Increasing the Schmidt number reduces mass diffusivity, which reduces the concentration distribution.
- The combined impacts of porous-medium resistance, variable thermal conductivity and chemical reaction have a considerable impact on momentum, temperature and concentration boundary layers, highlighting their relevance in governing transport processes in reactive non-Newtonian fluids.

Data Availability Statement

The findings of this work are based on theoretical analysis; no external data were required. Hence, all data generated or analysed during this study are included in this article.

References

1. F. Arpino, N. Massarotti, and A. Mauro, *A Stable Explicit Fractional Step Procedure for the Solution of Heat and Fluid Flow through Interfaces between Saturated Porous Media and Free Fluids in Presence of High Source Terms*, International Journal for Numerical Methods in Engineering, **83**(6) (2010), 671-–692.
2. R. A. Damseh, M. Q. Al-Odat, A. J. Chamkha and B. A. Shannak, *Combined Effect of Heat Generation or Absorption and First-Order Chemical Reaction on Micropolar Fluid Flows over a Uniformly Stretched Permeable Surface*, International Journal of Thermal Sciences, **48**(8) (2009), 1658-–1663.
3. M. Gnaneswara Reddy, *Unsteady Radiative-Convective Boundary-Layer Flow of a Casson Fluid with Variable Thermal Conductivity*, Journal of Engineering Physics and Thermophysics, **88**(1) (2015), 240-–251.
4. Y. Hirata, T. Dote, T. Yoshioka, Y. Komoda and Y. Inoue, *Performance of Chaotic Mixing Caused by Reciprocating a Disk in a Cylindrical Vessel*, Chemical Engineering Research and Design, **85**(5) (2007), 576-–582.
5. Y. Komoda, Y. Inoue, and Y. Hirata, *Characteristics of Laminar Flow Induced by Reciprocating Disk in Cylindrical Vessel*, Journal of Chemical Engineering of Japan, **34**(7) (2001), 919-–928.
6. Y. Lin, L. Zheng and X. Zhang, *Radiation Effects on Marangoni Convection Flow and Heat Transfer in Pseudo-Plastic Non-Newtonian Nanofluids with Variable Thermal Conductivity*, International Journal of Heat and Mass Transfer, **77** (2014), 708-–716.
7. Y. Lin, L. Zheng and G. Chen, *Unsteady Flow and Heat Transfer of Pseudo-Plastic Nanoliquid in a Finite Thin Film on a Stretching Surface with Variable Thermal Conductivity and Viscous Dissipation*, Powder Technology, **274** (2015), 324-–332.
8. R. A. Mahdi, H. A. Mohammed, K. M. Munisamy and N. H. Saeid, *Review of Convection Heat Transfer and Fluid Flow in Porous Media with Nanofluid*, Renewable and Sustainable Energy Reviews, **41** (2015), 715-–734.
9. S. Mukhopadhyay, P. R. De, K. Bhattacharyya and G. C. Layek, *Casson Fluid Flow over an Unsteady Stretching Surface*, Ain Shams Engineering Journal, **4**(4) (2013), 933-–938.
10. P. M. Patil, and P. S. Kulkarni, *Effects of Chemical Reaction on Free Convective Flow of a Polar Fluid through a Porous Medium in the Presence of Internal Heat Generation*, International Journal of Thermal Sciences, **47**(8) (2008), 1043-–1054.
11. Y-C. Pei, Q-C. Tan, F-S. Zheng and Y-Q. Zhang, *Dynamic Stability of Rotating Flexible Disk Perturbed by the Reciprocating Angular Movement of Suspension–Slider System*, Journal of Sound and Vibration, **329**(26) (2010), 5520-–5531.
12. S. Pramanik, *Casson Fluid Flow and Heat Transfer Past an Exponentially Porous Stretching Surface in Presence of Thermal Radiation*, *Ain Shams Engineering Journal*, **5**(1) (2014), 205-–212.
13. K. Ramesh, and M. Devakar, *Some Analytical Solutions for Flows of Casson Fluid with Slip Boundary Conditions*, Ain Shams Engineering Journal, **6**(3) (2015), 967–975.
14. S. A. Shehzad, T. Hayat, M. Qasim and S. Asghar, *Effects of Mass Transfer on MHD Flow of Casson Fluid with Chemical Reaction and Suction*, Brazilian Journal of Chemical Engineering, **30** (2013), 187-–1895.

15. T. Sochi, *Flow of Non-Newtonian Fluids in Porous Media*, Journal of Polymer Science Part B: Polymer Physics, **48** (2010), 2437-–2767. https://doi.org/10.1002/polb.22144.

S. Prasanna Rani: Department of Mathematics, ABV Government Degree College, Jangaon-506 167, Telangana, India.
Email address: prasannaradhakrishna28@gmail.com